THE JOURNAL OF BIOLOGICAL CHEMISTRY VOL. 292, NO. 7, pp. 2557–2570, February 17, 2017

Physiological Exploration of the Long Term Evolutionary Selection against Expression of *N*-Glycolylneuraminic Acid in the Brain*◆

Received for publication, November 18, 2016, and in revised form, December 26, 2016 Published, JBC Papers in Press, January 3, 2017, DOI 10.1074/jbc.M116.768531

Yuko Naito-Matsui[‡1], Leela R. L. Davies[‡], Hiromu Takematsu[‡§], Hsun-Hua Chou[‡], Pam Tangvoranuntakul[‡], Aaron F. Carlin[‡], Andrea Verhagen[‡], Charles J. Heyser[¶], Seung-Wan Yoo[‖], Biswa Choudhury[**], James C. Paton[‡‡], Adrienne W. Paton[‡‡], Nissi M. Varki[§§], Ronald L. Schnaar[¶¶], and Ajit Varki[‡2]**

*From the [‡]Departments of Medicine and Cellular and Molecular Medicine, [¶]Neuroscience Behavioral Testing Core, **Glycobiology Research and Training Center, and [§§]Department of Pathology, University of California San Diego, La Jolla, California 92093-0687, the [§]Department of Human Health Sciences, Graduate School of Medicine, Kyoto University, Sakyo, Kyoto 606-8507, Japan, the Departments of [‖]Neurology and [¶¶]Pharmacology and Neuroscience, The Johns Hopkins University School of Medicine, Baltimore, Maryland 21205, and the [‡‡]Research Centre for Infectious Diseases, Department of Molecular and Cellular Biology, School of Biological Sciences, University of Adelaide, Adelaide SA 5005, Australia*

Edited by Amanda J. Fosang

All vertebrate cell surfaces display a dense glycan layer often terminated with sialic acids, which have multiple functions due to their location and diverse modifications. The major sialic acids in most mammalian tissues are *N*-acetylneuraminic acid (Neu5Ac) and *N*-glycolylneuraminic acid (Neu5Gc), the latter being derived from Neu5Ac via addition of one oxygen atom at the sugar nucleotide level by CMP-Neu5Ac hydroxylase (Cmah). Contrasting with other organs that express various ratios of Neu5Ac and Neu5Gc depending on the variable expression of Cmah, Neu5Gc expression in the brain is extremely low in all vertebrates studied to date, suggesting that neural expression is detrimental to animals. However, physiological exploration of the reasons for this long term evolutionary selection has been lacking. To explore the consequences of forced expression of Neu5Gc in the brain, we have established brain-specific *Cmah* transgenic mice. Such Neu5Gc overexpression in the brain resulted in abnormal locomotor activity, impaired object recognition memory, and abnormal axon myelination. Brain-specific *Cmah* transgenic mice were also lethally sensitive to a Neu5Gc-preferring bacterial toxin, even though Neu5Gc was overexpressed only in the brain and other organs maintained endogenous Neu5Gc expression, as in wild-type mice. Therefore, the unusually strict evolutionary suppression of Neu5Gc expression in the vertebrate brain may be explained by evasion of negative effects on neural functions and by selection against pathogens.

Glycan structures expressed on cell surfaces are highly diverse, depending on species, cell type, cellular differentiation, and activation. These glycans on proteins or lipids are not just modifications of core molecules that can be utilized as markers of particular cells but also have independent functions via specific interaction with glycan-recognizing molecules, such as lectins (1–3). Thus, impairment of proper glycosylation gives rise to developmental abnormalities or diseases (4, 5).

Sialic acids are a family of monosaccharides that often occupy the non-reducing terminal position of vertebrate glycans. The lethal phenotype of mice gene-disrupted for UDP-GlcNAc 2-epimerase, a key enzyme of sialic acid biosynthesis, indicates that sialylation is essential for early development (6). Sialic acids serve as key determinants of various molecular recognition events because of their location at the outermost part of the cell surface and their structural diversity by molecular modification (3). In addition to endogenous sialic acid-binding molecules, *e.g.* sialic acid-binding immunoglobulin-like lectins (siglecs) (7, 8) or selectins (9), exogenous sialic acid receptors are also very common, such as those detected by bacterial adhesins or viral agglutinins (10–12).

The brain is known to be rich in sialic acids. Moreover, sialoglycans in the brain have unique features in their structure and sialic acid composition. The majority of brain sialic acids are in lipid-bound form, *i.e.* gangliosides (13). Gangliosides are involved in signal transduction as constituents of lipid rafts, mediate axon-myelin interactions, and support pathogenic infection by serving as receptors for neurotropic bacterial toxins (13). Another characteristic of sialylated glycan structure in the brain is polysialic acid (polySia),[3] a homopolymer of >90

* This work was supported by National Institutes of Health Grants R01GM32373 (to A. Varki) and R37NS037096 (to R. S.), the Mathers Foundation of New York (to A. Varki), and by a fellowship from the Japan Society for the Promotion of Science (to Y. N.-M.). The authors declare that they have no conflicts of interest with the contents of this article. The content is solely the responsibility of the authors and does not necessarily represent the official views of the National Institutes of Health.

◆ This article was selected as one of our Editors' Picks.

[1] Present address: Dept. of Biochemistry, Kobe Pharmaceutical University, Higashinada, Kobe 658-8558, Japan.

[2] To whom correspondence should be addressed: Depts. of Medicine and Cellular and Molecular Medicine, University of California, San Diego, La Jolla, CA 92093-0687. Tel.: 858-534-2214; Fax: 858-534-5611; E-mail: a1varki@ucsd.edu.

[3] The abbreviations used are: polySia, polysialic acid; Cmah, CMP-*N*-acetylneuraminic acid hydroxylase; MAG, myelin-associated glycoprotein; Neu5Ac, *N*-acetylneuraminic acid; Neu5Gc, *N*-glycolylneuraminic acid; Tg, transgenic; MBP, myelin basic protein; DMB, 1,2-diamino-4,5-methylenedioxybenzene; EndoNF, endo-*N*-acyl-neuraminidase derived from bacteriophage K1F; PNGase F, peptide:*N*-glycosidase; NSE, neuron-specific enolase.

sialic acid residues attached to selected proteins (13, 14). PolySia modulates cell-cell interactions, thus playing important roles in neuronal development and regeneration (15–17). Recently, it was suggested that polySia also serves as a reservoir of growth factors (18, 19). Genetic studies have revealed that variation in a gene encoding the enzyme that biosynthesizes polySia, *ST8SIA2,* could be a risk factor of psychiatric disorders such as schizophrenia, autism spectrum, and bipolar disorder (20–23).

Regarding sialic acids in the brain, there is one strikingly unusual feature of composition. In most mammals, the major sialic acids are *N*-acetylneuraminic acid (Neu5Ac) and *N*-glycolylneuraminic acid (Neu5Gc), which differ by only one oxygen atom at the C-5 *N*-acyl group (24). Neu5Gc is biosynthesized from Neu5Ac as a sugar nucleotide donor. This conversion from CMP-Neu5Ac to CMP-Neu5Gc in the cytosol is catalyzed by CMP-Neu5Ac hydroxylase (Cmah) (25, 26). The ratio of the cytosolic CMP-Neu5Ac and CMP-Neu5Gc pool likely determines the Neu5Ac/Neu5Gc ratio in cell surface sialoglycans, because the Golgi CMP-sialic acid transporter and sialyltransferases can utilize both CMP-Neu5Ac and CMP-Neu5Gc as substrates without strong preferences (27–29). Because of the differential regulation of Cmah expression, the ratio of these two major sialic acids varies markedly among different tissues in different animal species except for certain species like humans that have an inactive *CMAH* gene (*CMAHP*) and lack endogenous Neu5Gc expression throughout the body. Even in species that express ample Neu5Gc in other tissues, the brain shows extremely low Neu5Gc expression (<3%) in all vertebrate species tested to date, from fish to chimpanzees (30, 31). In other words, the suppression of Neu5Gc expression in the vertebrate brain appears to be universal to all vertebrates studied so far, regardless of highly variable expression in other cell types (30). This stringent conserved evolutionary brain expression pattern suggests possible negative effects of Neu5Gc on neural development and/or function.

In this study, we generated Neu5Gc-overexpressing *Cmah* transgenic (Tg) mice to address the physiological significance of Neu5Gc suppression in the vertebrate brain. We applied a Cre-*loxP* system to allow controlled expression of transgene-derived Cmah by Cre recombinase. *Cmah* Tg mice obtained by crossing such mice with brain-specific Cre mice showed high and widely distributed Neu5Gc expression in the whole brain. Success in establishing *Cmah* Tg mice with high Neu5Gc expression allowed us to examine the consequences of Neu5Gc expression in the brain. We report both neural abnormalities and increased sensitivity to a Neu5Gc-preferring bacterial toxin, findings that could explain the consistent evolutionary suppression of Neu5Gc in the vertebrate brain.

Results and Discussion

Trace Amounts of Neu5Gc Reported in Vertebrate Brains Are Primarily in Endothelial Cells—Biochemical analyses found very low amounts of Neu5Gc (<3%) in all vertebrate brains tested to date even in species that express high levels of Neu5Gc in other tissues (30). We used a sensitive and specific antibody that reacts with all known Neu5Gc-containing epitopes (32) to probe frozen sections of brains from multiple vertebrates that are known to express Neu5Gc in other tissues. We found that even this small amount of Neu5Gc is mostly expressed on the endothelial lining of blood vessels. Fig. 1 shows the results with mouse brain. Similar selective expression of Neu5Gc in an endothelial pattern was seen in brain sections from chimpanzees, rabbits, rats, *Xenopus*, and whitefish (data not shown). Not all the blood vessels in rabbit and rat brain sections had strong expression of Neu5Gc, and some macrophages/microglia in these species showed expression (data not shown). Regardless, no species studied showed clear staining of neural cells or the neuropil.

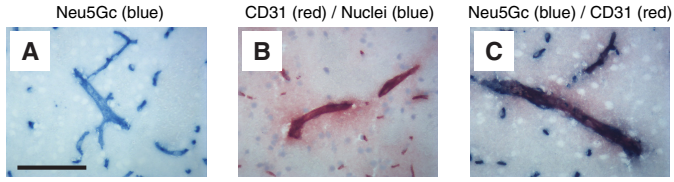

FIGURE 1. **Neu5Gc expression on endothelium lining blood vessels in the brain.** Frozen brain sections were stained with chicken anti-Neu5Gc antibody (*A*), anti-CD31 antibody (*B*), or both antibodies (*C*). *B* (anti-CD31 staining), nuclei were counterstained with Mayer's hematoxylin (*blue*). *Scale bar* = 100 μm. Data are representative of multiple independent experiments that yielded similar results.

Lethality Observed in Initial Attempts to Overexpress Cmah in the Developing Embryo—To explore the evolutionary advantage of this specific and extreme suppression of Neu5Gc in vertebrate brain for hundreds of millions of years of evolution, we first tried to make mice with increased Neu5Gc in the brain by forced expression of the *Cmah* cDNA encoding the enzyme responsible for Neu5Gc biosynthesis. In the initial attempts, cytomegalovirus (CMV) promoter or neuron-specific enolase (NSE) promoter was used to express transgene-derived *Cmah* in a systemic or neuron-specific manner, respectively (33). In both instances, no live mice with Neu5Gc expression in the brain were obtained (Table 1). Even the few transgene-positive mice that were born did not express *Cmah* mRNA in the brain, suggesting that Neu5Gc expression might be lethal. When a *Cmah* frameshift mutation was introduced into the NSE promoter construct, a higher (typically expected for the transgenic facility) rate of live births was seen. Also, as expected, the mutant mRNA was expressed in the brain with no increase in Neu5Gc expression, indicating that suppression of Cmah expression in the brain is not due to mRNA instability. To investigate the mechanism of this apparent lethality, development of embryos after the CMV-promoter transgene injection was checked at embryonic day E13.5. Ninety percent of transgene-positive mice showed abnormalities such as being eyeless or decomposition of embryos (Fig. 2), suggesting toxicity of the construct-mediated overexpression at some earlier stage of development.

Success in Obtaining Live Mice with Neu5Gc Overexpression in the Brain—In view of these findings, Tg mice harboring a Cre-inducible system for *Cmah* expression were generated (Fig. 3*A*). Mating of mice having an inducible *Cmah* transgene with synapsin-*Cre*-positive mice was used to selectively induce *Cmah* expression in neurons (34, 35). Live mice with high

TABLE 1

Results of initial attempts to produce transgenic mice with brain expression of Neu5Gc

Cmah cDNA was expressed under CMV promoter or NSE promoter. With the NSE promoter, a frameshift mutant *Cmah* cDNA was also tried. The numbers of live births and transgene-positive mice were indicated.

Promoter	*Cmah* cDNA	Live births	Founders (transgene-positive)	Transmitted to F1	Message expression in brain[a]	Increased Neu5Gc in brain
CMV	Wild type (active)	105	4	4	No	No
NSE	Wild type (active)	72	2	2	No	No
NSE	Mutant[b] (inactive)	57	9	6	Yes (5)	No

[a] The endogenous message is positive in liver.
[b] Single base pair frameshift mutation is in coding sequence of *Cmah*.

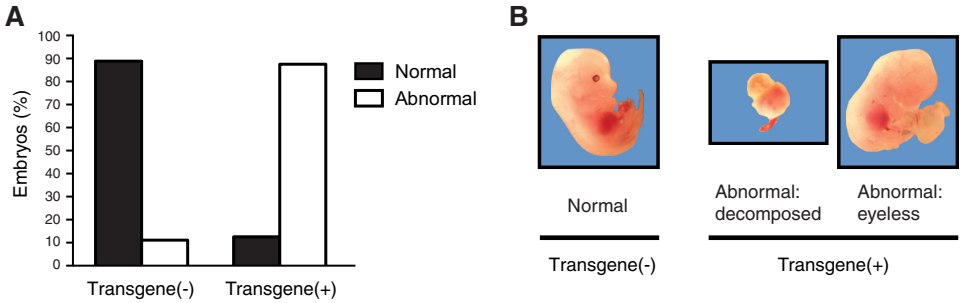

FIGURE 2. **Direct observation of *Cmah* transgenic embryos with CMV promoter.** Fertilized mouse eggs were injected with purified plasmids encoding *Cmah* cDNA downstream of a CMV promoter and implanted in pseudo-pregnant mice. At E13.5 stage, 90% of embryos with *Cmah* transgene demonstrated abnormal phenotypes (*A*), including absence of eyes or decomposition of embryo as shown in *B*. $n = 18$.

Neu5Gc expression in the brain were obtained from three Tg founders (data not shown). We picked the Tg mouse founder line that showed the highest Neu5Gc expression with synapsin-*Cre* and crossed it with a nestin-*Cre* mouse, which induced transgene expression at an earlier stage and in a broader range of cells in the brain than synapsin-*Cre* (36). Again, live mice expressing Cmah in the brain were obtained. In this case, the Neu5Gc/Neu5Ac ratio in their brains reached more than 80% (Fig. 3*B*), and Cmah expression was confirmed by Western blotting (Fig. 3*C*). Anti-Neu5Gc blotting revealed that Neu5Gc was incorporated into multiple proteins (Fig. 3*D*). Immunohistochemistry of brain sections using anti-Neu5Gc antibody showed Neu5Gc expression throughout the brain (Fig. 3*E*). Thus, lack of lethality in synapsin-*Cre Cmah* Tg and nestin-*Cre Cmah* Tg mice was not a result of Neu5Gc expression in a limited (tolerant) area of the brain.

The discrepancy with the original evidence for lethality could be due to earlier expression of those transgenes during development (the NSE promoter was later found to be "leaky"). However, even when we made mice expressing the transgene-derived *Cmah* gene in preimplantation mouse embryos by mating Cre-inducible *Cmah* Tg mice with EIIa-*Cre* mice (37), animals with high Neu5Gc were born in predicted Mendelian inheritance ratios (data not shown). From these results, we concluded that Neu5Gc expression in early embryos or in the brain is not lethal. The lethality in our initial attempts may have been due to the classical transgenic techniques used involving injection of ~1000 copies of a complete transcriptional unit for Cmah production (38). A transient high expression of the enzyme following the injection may have temporarily affected the embryo either directly or by depleting one or more of the known enzyme co-factors, such as iron, oxygen, NADH, or cytochrome b_5 reductase-cytochrome b_5 (39). Given the possibility of such an artifact, we focused instead on the impact of Neu5Gc in the brain of the live mice that were generated using the Cre-inducible method.

No Gross Defect in Development or Fertility of Cmah-overexpressing Mice—Establishment of live brain Neu5Gc-overexpressing mice allowed us to study the effects of Neu5Gc expression on development and brain function. The nestin-*Cre* mouse was chosen as the best way to drive brain-specific transgene expression (hereafter called N*Cmah*Tg mice). Transgene-positive mice were born in the accordance with Mendelian inheritance ratios (Fig. 3*F*). No gross defect was observed in fertility, development, and brain size (Fig. 3*G*), although the brains of N*Cmah*Tg mice appeared slightly narrow (data not shown).

Effect of Neu5Gc Overexpression on Polysialylation—PolySia is a long chain of sialic acids attached to a limited set of proteins such as NCAM and SynCAM1 found mostly in the brain and especially in the developing brain (15, 40, 41). NCAM is the most studied polysialylated protein. Polysialylated NCAM plays important roles not only in cell-cell interactions but also as a reservoir of brain-derived neurotrophic factor or growth factors to release them upon polySia degradation (18). Because polySia is mainly expressed in the brain (where Neu5Gc is not normally expressed), it has been only studied in a Neu5Ac form. Previously, we reported that Neu5Gc incorporation into the polySia chain slows polySia degradation by sialidases and suggested that this might affect brain development and function (30). Thus, we checked Neu5Gc incorporation into brain polySia by HPLC. PolySia from postnatal day 1 N*Cmah*Tg mouse brain contained 68% of Neu5Gc, whereas control mouse polySia had only about 2% (Fig. 4*A*). Polysialylation of NCAM was also analyzed by immunoblotting. Given that the currently available anti-polySia antibodies have a strong preference for either Neu5Ac or Neu5Gc (30), we used an anti-NCAM antibody to detect polysialylated NCAM (Fig. 4*B, left*). N*Cmah*Tg

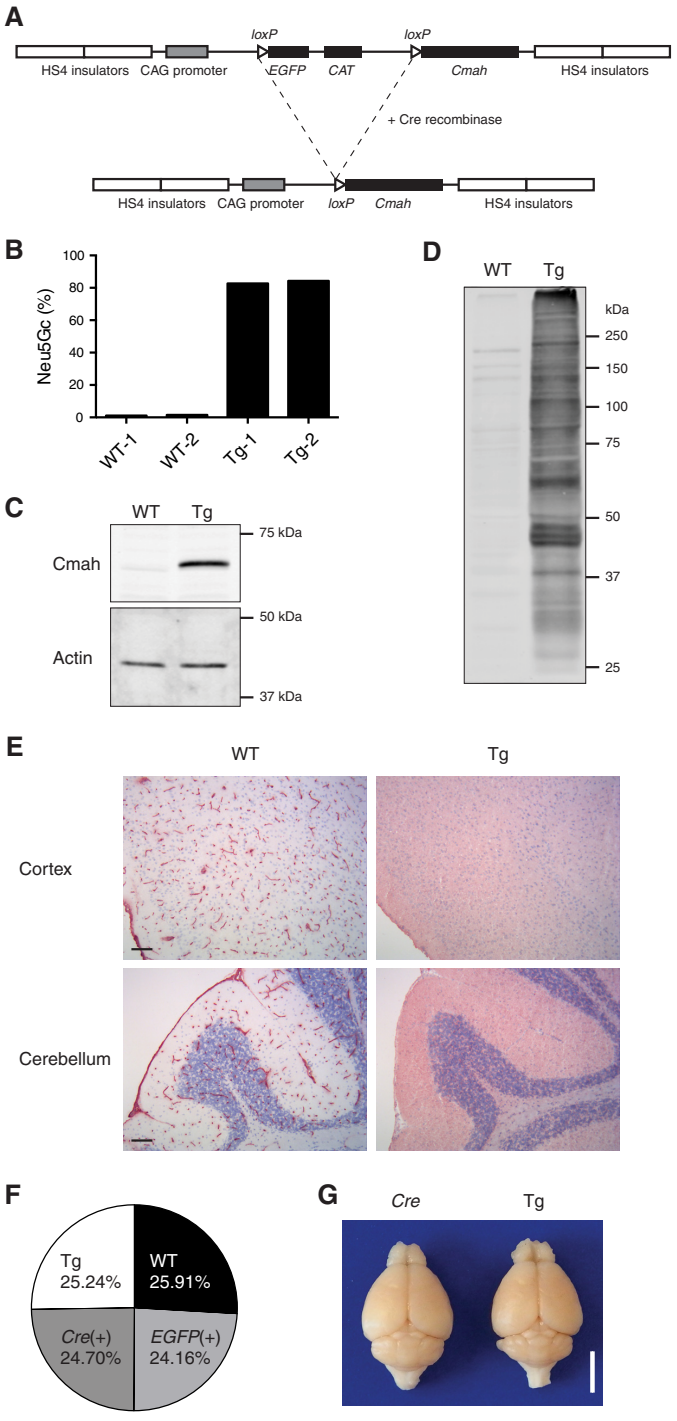

FIGURE 3. **Establishment of Neu5Gc-overexpressing *Cmah* Tg mice.** *A*, construct for Cre-inducible transgenic *Cmah* expression. In the presence of Cre recombinase, the floxed *EGFP* gene is eliminated, and the *Cmah* gene is expressed under a strong CAG promoter. *B*, Neu5Gc expression in nestin-*Cre*-positive *Cmah* Tg mice (NC*mah*Tg). Neu5Gc% in total sialic acids of brain lysate was determined by acid release, DMB derivatization, and HPLC. Each *bar* represents result obtained from an independent animal. *C*, transgene-derived Cmah expression in NC*mah*Tg mice. Cmah expression was examined by Western blotting. *D*, Neu5Gc incorporation into various proteins. Neu5Gc-containing sialoglycoproteins were detected by Western blotting using chicken anti-Neu5Gc IgY. *E*, immunohistochemical detection of Neu5Gc in the brain. Frozen brain sections were stained with chicken anti-Neu5Gc IgY and visualized with HRP substrate (*red*). Nuclei were counterstained with Mayer's hematoxylin (*blue*). *Scale bar* = 100 μm. *F*, birth ratios of transgenic mice. The ratios of wild-type (WT), *Cmah* transgene only (*EGFP*(+)), *Cre* only (*Cre*(+)), and *Cmah* transgene-positive *Cre*-positive NC*mah*Tg (Tg) mice among a total of 741 mice are shown. *G*, brains from 6-month-old mice after perfusion-fixation. *Scale bar* = 5 mm. *WT*, wild-type; Cre, *Cre*-positive (no *Cmah* transgene); *Tg*, NC*mah*Tg. Data are representative of multiple independent experiments that yielded similar results.

mice expressed polysialylated NCAM, which was detected as high molecular weight smeared bands, at an almost comparable level as control, although the length of polySia may be slightly shorter. These smeared bands in control samples were positively detected by anti-polySia antibody, which barely detected Neu5Gc-containing polySia bands in the NC*mah*Tg sample because of its strong preference to Neu5Ac (Fig. 4*B, right*). Polysialylation of these smeared bands was confirmed by cleaving polySia chains with EndoNF. It should be noted that EndoNF worked less effectively on Neu5Gc, which might result in the difference in Neu5Gc% of total lysate and EndoNF-released polySia in Fig. 4*A*. NCAM expression was comparable with control, because *N*-glycan removal by PNGase F treatment gave NCAM bands (140 and 180 kDa) with similar intensity. Thus, Neu5Gc is incorporated into NC*mah*Tg polySia as well as Neu5Ac, and yet apparently it results in no gross defect in brain development. Of course, this does not rule out the possibility that neuronal development might be affected at the cellular level or that the release of brain-derived neurotrophic factor or growth factors bound on polySia might be impaired (19).

Loss of Myelin-associated Glycoprotein (MAG) Ligand and Abnormal Myelination in NCmahTg Mice—Another feature of sialoglycan expression characteristic to the brain is the relatively large amount of gangliosides (13). Indeed, most studies with gangliosides are done with Neu5Ac-containing gangliosides purified from the brain. Thus, there is not much knowledge to predict how Neu5Gc incorporation affects ganglioside function. One candidate molecule that can be impacted by the change in sialic acid species from Neu5Ac to Neu5Gc is myelin-associated glycoprotein (MAG, Siglec-4) (42). MAG is a sialic acid-binding protein expressed on myelin (innermost layer of myelin) and is known to prefer Neu5Ac to Neu5Gc for its ligand (43, 44). MAG is considered to mediate tight interactions between axon and myelin and axonal outgrowth via its binding to glycan ligands and protein-protein interaction (42, 45). *Mag*-null mice and *B4galnt1* (β-1,4-*N*-acetylgalactosaminyltransferase 1)-null mice lacking complex gangliosides, which have been used as MAG ligand-deficient mice, showed dysmyelination especially as they aged (46–49). *B4galnt1*-null mice lack MAG glycan ligands; nevertheless, they cannot fully reveal MAG ligand function because they lack complex gangliosides that could have important functions independent from those as MAG ligands and instead increase simple gangliosides. We asked whether NC*mah*Tg mice had reduced MAG ligands without affecting ganglioside composition except for sialic acid species and showed similar phenotypes as *Mag*-null mice and *B4galnt1*-null mice. First, Neu5Gc incorporation into ganglioside was confirmed by mass spectrometry (Fig. 5*A*). Then, MAG glycan ligand expression was examined by staining frozen brain sections with MAG-Fc, a chimeric probe consisting of the first three domains of MAG and the Fc region of human IgG. Very little binding was observed in NC*mah*Tg mice, indi-

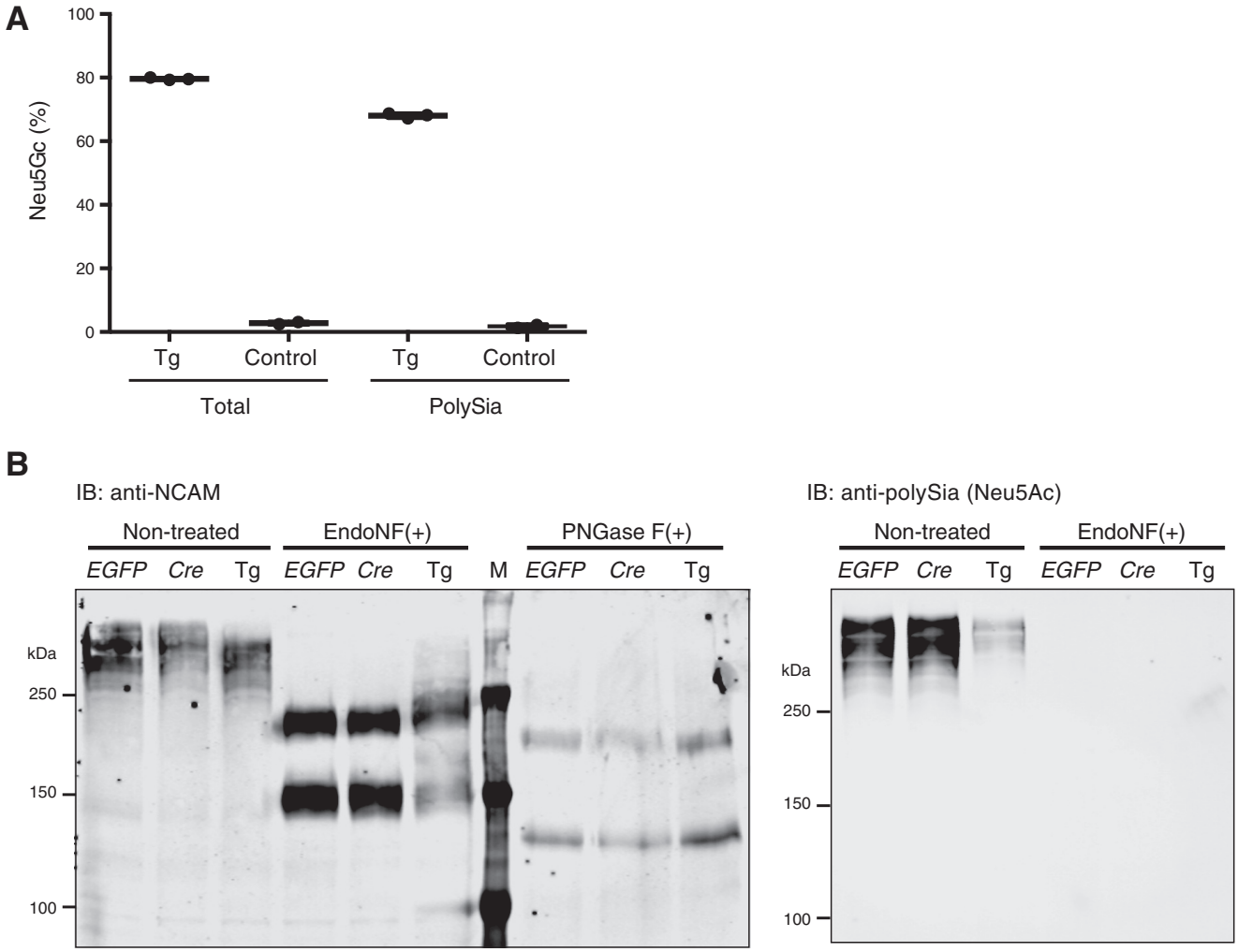

FIGURE 4. **Neu5Gc expression on polysialylated proteins.** *A*, Neu5Gc incorporation into polySia. Delipidated brain homogenate from postnatal day 2–3 mice (littermates) was treated with EndoNF, and the released polySia-derived oligoSia fragments were hydrolyzed in acetic acid for DMB derivatization. Neu5Gc/Neu5Ac ratio in the obtained polySia-derived fractions (*PolySia*) or the delipidated homogenate before EndoNF treatment (*Total*) was analyzed by HPLC. *Control*, *Cmah* transgene-positive (no *Cre*) or *Cre*-positive (no *Cmah* transgene); *Tg*, N*Cmah*Tg. Each *dot* represents an individual animal, and *bars* indicate the means. *B,* expression of polysialylated NCAM. Brain lysate from postnatal day 1 mice were treated with EndoNF or PNGase F to cleave polySia or *N*-glycan, respectively, and then subjected to Western blotting with anti-NCAM (*left*) or anti-Neu5Ac polySia (*right*) antibodies. *EGFP*, *Cmah* transgene-positive (no *Cre*); *Cre*, *Cre*-positive (no *Cmah* transgene); *Tg*, N*Cmah*Tg; *M*, molecular weight marker; *IB*, immunoblot. Data are representative of two independent experiments that yielded similar results.

cating that N*Cmah* Tg mice lacked MAG glycan ligands (Fig. 5*B*).

Although MAG is not required for myelination itself, it is thought to help with preserving myelinated structures and protecting axons. Indeed, disruption of MAG-ligand interactions results in dysmyelination (48–50). Thus, EM imaging was done for corpus callosum, the major myelinated axon tract in the central nervous system (Fig. 6). Thinly myelinated and unmyelinated large axons were observed in cross-sections of the corpus callosum of N*Cmah* Tg mice compared with control mice. In the peripheral nervous system, light microscope images of the entire cross-section of the sciatic nerve revealed increased axon degeneration in N*Cmah*Tg mice compared with control mice (Fig. 7).

Because abnormal myelination causes impaired motor coordination and balance, a hindlimb extension test, one of the methods to assess neuropathy, was performed using aged mice over 1 year old (Fig. 8*A*). The formal score of hindlimb reflex extension did not show a significant difference between N*Cmah*Tg and control mice. Nonetheless, the response of N*Cmah*Tg mice seemed to be different from control mice, upon close observation. Thus, severity was evaluated by adding two more factors, the behavior of pulling the hindlimbs to the body (some mice occasionally pulled their hindlimbs close to the body even though they still could extend hindlimbs) and loss of finding a stable position of hindlimb (normal mice usually find a comfortable angle to keep their hindlimbs extending soon after suspension) (Fig. 8*B*). In these analyses, the severity score was higher in male N*Cmah*Tg mice than control mice, indicating mild impairment of myelination, which is consistent with EM imaging results (Figs. 6 and 7). To further analyze effects of Neu5Gc expression on motor function, gait analysis, rotarod, and activity testing were performed using aged mice. The results of the gait analysis showed that the stride length of N*Cmah*Tg mice was shorter than control mice, although the distance between paws was not different from control (Fig. 8, *C* and *D*). No differences were observed in an accelerating rotarod test that assesses both motor function and motor

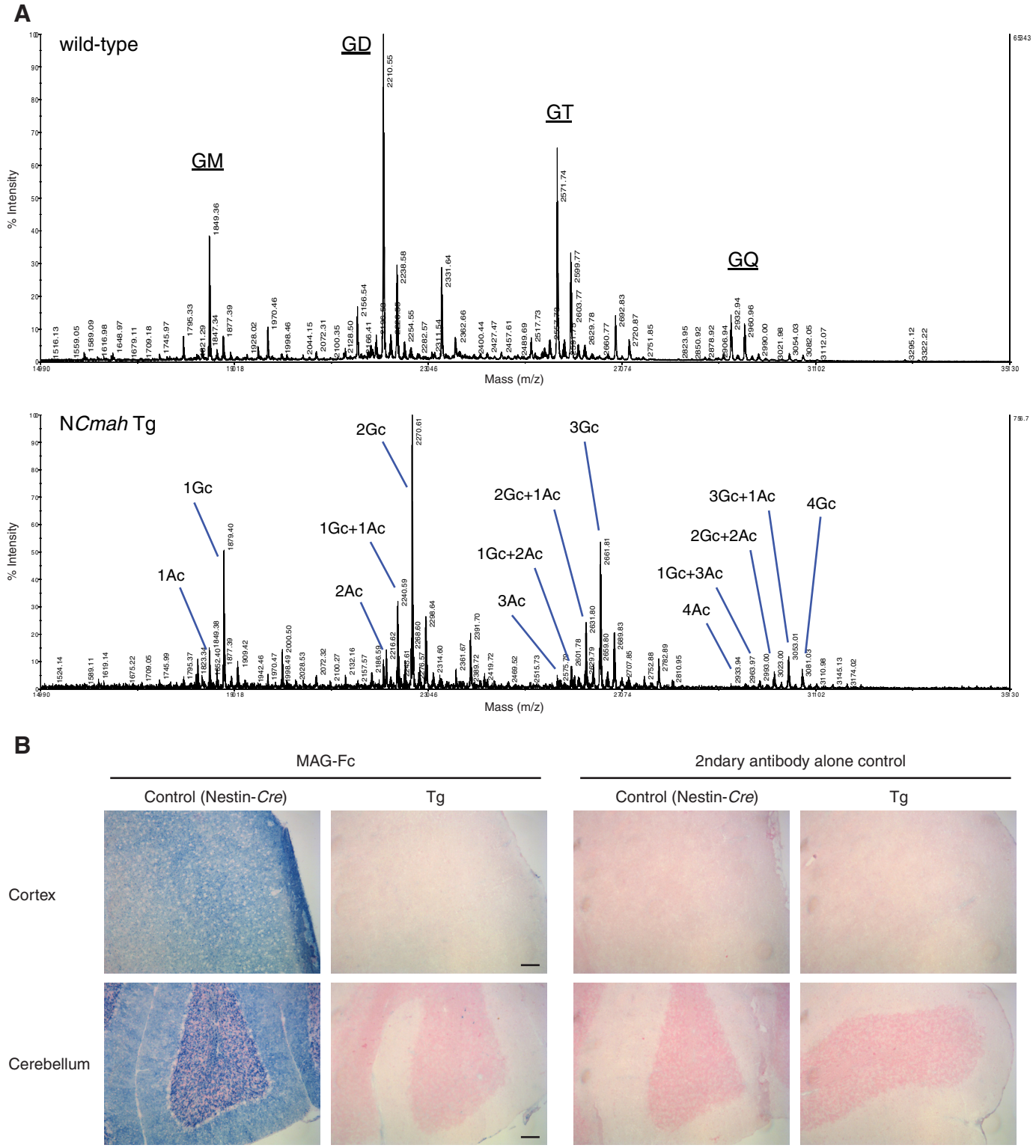

FIGURE 5. **Loss of MAG ligand(s) in NC*mah*Tg mice.** *A,* mass spectrum of brain gangliosides. Gangliosides extracted from wild-type and NC*mah*Tg mouse brains were analyzed by MALDI-TOF/TOF to examine Neu5Gc incorporation into mono- (*GM*), di- (*GD*), tri- (*GT*), and tetra-sialyl (*GQ*) gangliosides. *Ac*, Neu5Ac; *Gc*, Neu5Gc. Data are representative of the results obtained from two mice per genotype. *B,* frozen brain sections from 10-month-old mice were stained with MAG-Fc chimeric probe precomplexed with alkaline phosphatase-conjugated anti-human IgG (*blue*). Nuclei were counterstained with Nuclear Fast Red (*red*). *Tg*, NC*mah*Tg. *Scale bar* = 100 μm. Data are representative of three independent experiments that yielded similar results.

learning (Fig. 8*E*). NC*mah*Tg mice exhibited hyperactivity throughout the test time in this study (Fig. 8*F*), consistent with a previous report showing that *Mag*-null and *B4galnt1*-null mice were reported to be hyperactive (49). Basal pain response was also assessed given that it can be mediated by myelinated axons. NC*mah*Tg mice exhibited normal thermal nociception sensitivity in the hot plate test (Fig. 8*G*). Taken together, the results suggested that the impairment of

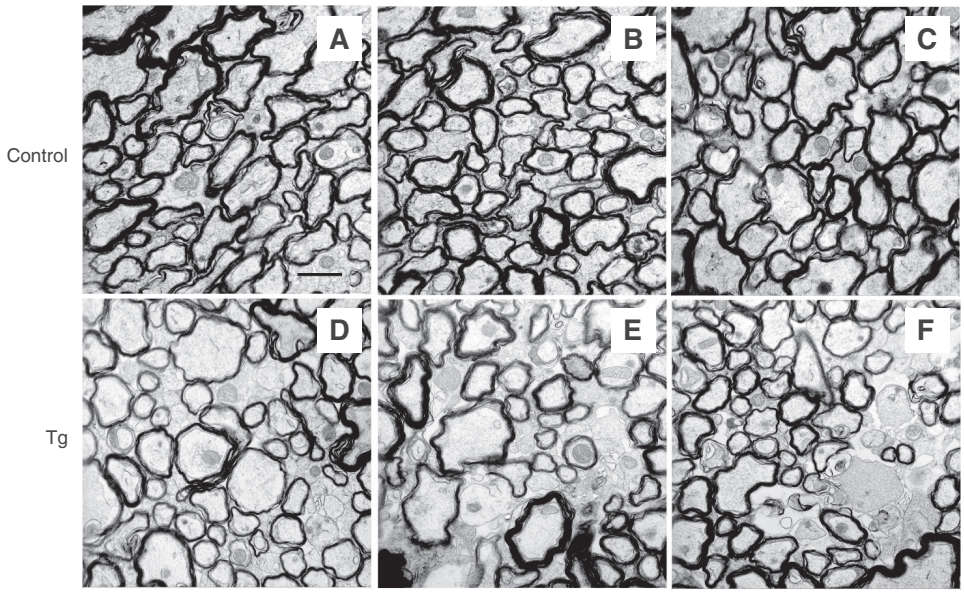

FIGURE 6. **Impaired myelination in the central nervous system of NC*mah*Tg mice.** EM imaging of myelination in cross-sections of the corpus callosum of 1.5-year-old mice revealed the presence of thinly myelinated or unmyelinated large axons. *A–C*, control (wild-type or *Cre*-positive (no *Cmah* transgene)); *D–F*, NC*mah*Tg. *Scale bar* = 1 μm. Data are representative of the results obtained from five mice per genotype in two independent experiments.

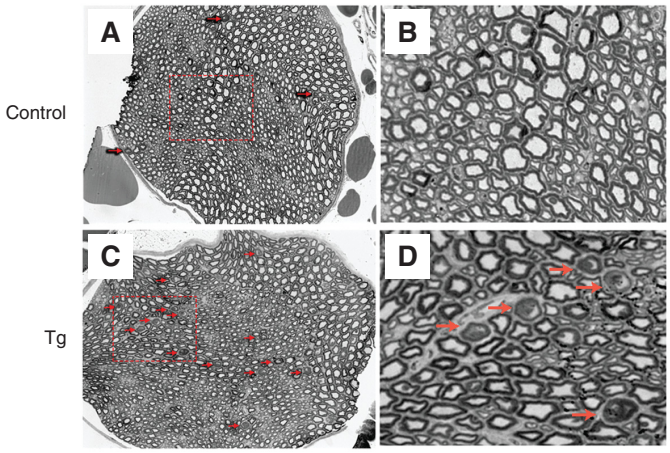

FIGURE 7. **Axon degeneration in the peripheral nervous system of NC*mah*Tg mice.** Light microscope images of cross-sections of toluidine blue-labeled sciatic nerves from control (wild-type or *Cre*-positive (no *Cmah* transgene)) mice (*A* and *B*) and NC*mah*Tg mice (*C* and *D*) revealed increased degeneration (*arrows*) in the NC*mah*Tg mice. *Boxed areas* in *A* and *C* are shown at higher magnification in the adjacent panels (*B* and *D*). Data are representative of the results obtained from two (control) or three (NC*mah*Tg) mice.

myelination was not severe and dysfunction was partly compensated. Nonetheless, the phenotypes found here under normal ganglioside composition (except for the change in sialic acid composition) indicated that MAG ligand is involved in proper myelination, and contribution of loss of complex gangliosides is minor.

Overall, NC*mah*Tg mice showed similar but milder phenotypes of neuropathy compared with *Mag*-null or *B4galnt1*-null mice. The remaining protein-protein interaction of MAG in NC*mah*Tg mice might contribute to this difference. Unlike the case of *B4galnt1*-null mice (51), MAG expression was not changed in NC*mah*Tg mice, which might explain the relatively milder impairment of myelin structure (Fig. 8*H*). Disruption of membrane ganglioside composition in *B4galnt1*-null mice might cause the decrease of MAG expression independently from the loss of MAG-glycan ligand interaction.

Behavioral Abnormalities of NCmahTg Mice—Because sialic acid is attached to a variety of glycoproteins throughout the brain, Neu5Gc overexpression could affect multiple brain functions. Therefore, we focused on memory function and activity that are often affected in psychiatric disorders. The nestin-*Cre*-positive mice without the *Cmah* transgene were used as a control. First, locomotor activity was measured. Interestingly, in contrast to the hyperactivity in aged mice (Fig. 8*F*), NC*mah*Tg mice at the age of 5– 6 months were less active throughout a test time (120 min) compared with control mice (Fig. 9*A*). The habituation to the new environment was normal, because traveling distance decreased across time in both control and NC*mah*Tg mice. Neu5Gc expression dependence of this phenotype was confirmed by repeating the test using *Cmah* transgene-positive *Cre*-negative mice as a control group (data not shown).

Next, we assessed the effects of Neu5Gc overexpression on memory formation. In the Barnes maze test to assess spatial memory, NC*mah*Tg mice were not different from control mice, both in terms of latency to escape and error, suggesting that spatial memory is normal in Neu5Gc-overexpressing mice (Fig. 9, *B–D*). Recognition memory was examined using the novel object recognition test. In this test, NC*mah*Tg mice did not discriminate between familiar and novel objects, indicating that their recognition memory is impaired (Fig. 9, *E* and *F*). Given that the Barnes maze is more reliant on intact hippocampal function and novel object recognition relies on the perirhinal cortex (52, 53), additional tests aimed at brain localization were conducted. NC*mah*Tg mice were assessed in a fear-conditioning procedure that consisted of hippocampus-dependent contextual fear conditioning and amygdala-dependent cued fear conditioning. In tests of both contextual and cued fear conditioning, no difference was observed between control and

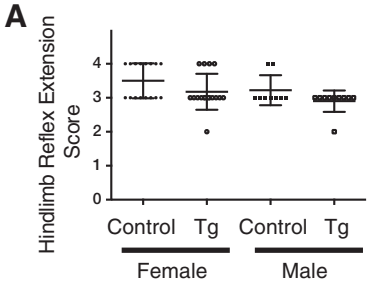

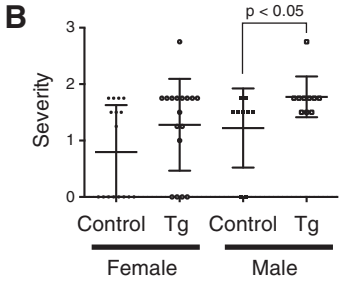

Severity	Score	Pulled leg(s) to body	Stable position
0	4	-	Yes (Y)
0.25	4	-	No (N)
0.5	4	+	Y
0.75	4	+	N
1	3	-	Y
1.25	3	-	N
1.5	3	+	Y
1.75	3	+	N
2	2	-	Y
2.25	2	-	N
2.5	2	+	Y
2.75	2	+	N
3	1	-	Y
3.25	1	-	N
3.5	1	+	Y
3.75	1	+	N

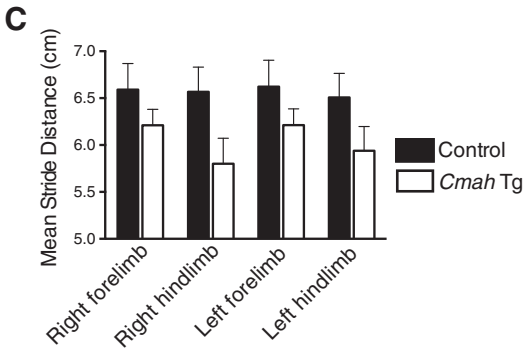

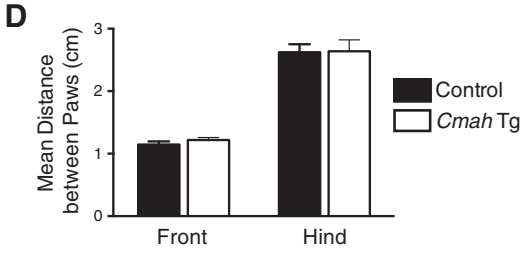

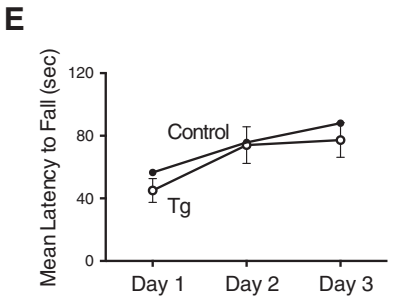

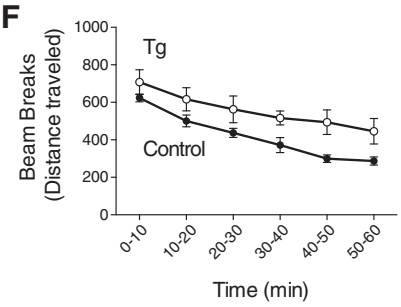

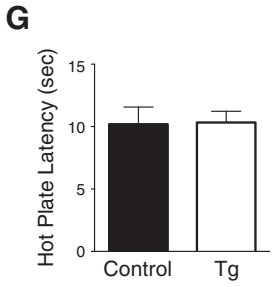

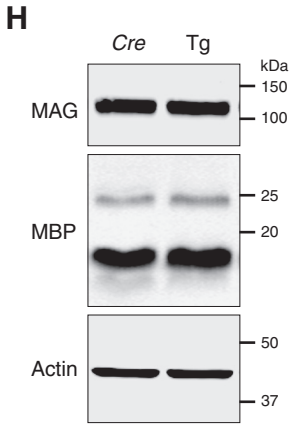

N*Cmah*Tg mice (Fig. 9*G*). Thus, these results suggest that Neu5Gc-containing sialoglycans can differentially regulate neural function in different areas of the brain. This is of great interest because overexpressed Neu5Gc seems to be expressed throughout the brain (Fig. 3*E*). Further studies could reveal region-specific function of sialoglycans in the brain. It should also be noted that the incorporation of Neu5Gc into polySia chains, whose expression seems to be regulated in a spatio-temporal manner, may contribute to these functional abnormalities.

Effect on Susceptibility to Bacterial Toxin—Given the near complete absence of Neu5Gc in the brains of all Cmah-positive vertebrates studied to date (31), it is reasonable to assume that the persistence of this strong suppression in so many lineages is due to some strong evolutionary selection factor(s). Although we found mild neural abnormalities of various kinds in the N*Cmah*Tg mice, none of these would seem to be detrimental enough by themselves to account for such strong selection. Another mutually non-exclusive possibility for selection that might favor Neu5Gc suppression in the brain is susceptibility to microbial toxins that bind to Neu5Gc-containing glycoconjugates. To examine this hypothesis, we used subtilase cytotoxin (SubAB toxin) that we earlier reported to show a high binding specificity for glycan receptors terminating in Neu5Gc rather than Neu5Ac (10). To deliver toxin efficiently to the brain, toxin was intranasally administered (54). Compared with the control group, N*Cmah*Tg mice were indeed more susceptible to SubAB toxin, indicating that Neu5Gc expression "in the brain" could affect resistance to infectious diseases "as individuals" (Fig. 10). Because transgene-derived Neu5Gc overexpression occurs only in the brain and Neu5Gc expression in other tissues is the same as that in control mice, this result strongly indicates the importance of differentiating possible targets of toxins in the brain from other tissues.

Conclusions and Perspectives—From the earliest days in which sialic acids were studied in the vertebrate brain, investigators have commented on the rarity of Neu5Gc in this otherwise sialic acid-rich organ (55, 56). The fact that expression is not at all tightly regulated in other tissues (30, 31) makes this observation all the more intriguing. Moreover, cells, including embryonic stem cells or primary cultured neurons, are usually cultured in medium containing fetal bovine serum, a source of Neu5Gc, suggesting that possibly toxic effects of Neu5Gc do not target individual neural cells but rather affect the overall central nervous system. Here, we have addressed this long-standing mystery about the evolutionary advantage of this specific and extreme suppression of Neu5Gc in neural tissues by demonstrating some detrimental consequences in *Cmah* transgenic mice. At first glance, the severity of the phenotypes cannot seem strong enough to provide an explanation. However, the brain is the most critical organ essential for survival and eventually for reproductive fitness. It remains to be seen whether there are other phenotypes, which we have not yet uncovered, that may be contributing to the selection. It would also be interesting to study the promoters and other genetic/epigenetic components responsible for the Cmah suppression. If the critical components can be identified, they could potentially be used to selectively suppress expression of other genes in the brain.

Experimental Procedures

Animals—Cmah Tg mice were established by the standard injection method. In initial attempts, purified plasmids with a cytomegalovirus (CMV) promoter or an NSE promoter 5′ to the *Cmah* cDNA were injected into fertilized mouse eggs, and surviving eggs were implanted in pseudo-pregnant mice. Cre-inducible *Cmah* transgene construct consists of CAG promoter, floxed *EGFP* and *CAT* genes, and mouse *Cmah* cDNA, which are flanked by HS4 insulators (57). Brain-specific *Cmah* Tg mice were obtained by crossing Cre-inducible *Cmah* Tg mice with synapsin-*Cre* mice (35) or nestin-*Cre* mice (36) after backcrossing to C57BL/6N. All animal experiments were performed in accordance with the Institutional Animal Care and Use Committee of University of California, San Diego.

Immunohistochemistry—Unfixed brain was frozen with OCT compound in a dry ice/isopentane and cryo-sectioned using a cryostat (10 μm thickness for Neu5Gc staining and 8 μm for MAG-Fc). For Neu5Gc staining, endogenous peroxidase activity was quenched with 0.03% hydrogen peroxide in phosphate-buffered saline containing 0.1% Tween 20 (PBS-T), and endogenous biotin was blocked with avidin-biotin blocking kit (Vector Laboratories). After fixation in 10% neutral buffered formalin for 30 min at room temperature, the sections were incubated in 0.5% fish gelatin-containing PBS-T to block non-specific binding and stained with chicken anti-Neu5Gc antibody (1:2000, BioLegend) for 1 h followed by biotinylated donkey anti-chicken IgY (1:500, Jackson ImmunoResearch) for 30 min and horseradish peroxidase-conjugated streptavidin (1:500, Jackson ImmunoResearch) for 30 min. The antibodies and probe were diluted in 0.5% fish gelatin-containing PBS-T, and all incubation was done at room temperature. The antibody binding was visualized using AEC peroxidase substrate kit (Vector Laboratories), and cell nuclei were counterstained with Mayer's hematoxylin. For Neu5Gc/CD31 double staining

FIGURE 8. **Analysis of neuropathic phenotypes in aged mice (1–1.5 years old).** *A* and *B,* hindlimb extension test. *A*, reflection of tail-suspended mice was observed for 30 s and scored based on the criteria described under "Experimental Procedures." Briefly, lower score means severe phenotype. *B*, two more factors were added to the score used in *A* to evaluate neuropathy phenotype (see under "Experimental Procedures"). The difference between male control and N*Cmah*Tg mice was significant when analyzed by two-tailed unpaired *t* test. Each *dot* represents an individual animal, and *bars* indicate the means with S.D. $n = 9$ (male control), 10 (male N*Cmah*Tg), 16 (female control), or 17 (female N*Cmah*Tg). *C* and *D,* gait analysis. Mean stride distance (centimeters) (*C*) and distance between the paws (centimeters) (*D*) with S.E. is shown. $n = 6$ (control) or 7 (N*Cmah*Tg). The difference in stride distance between control and N*Cmah*Tg mice was statistically significant when analyzed by two-way analysis of variance ($p = 0.0037$). *E,* rotarod test. Mean latency to fall (average of three trials per day) with S.E. was plotted. $n = 7$ (control) or 9 (N*Cmah*Tg). *F,* open field test. Locomotor activity was recorded for 1 h, and beam breaks (traveled distance) are plotted per 10 min. $n = 6$ (control, N*Cmah*Tg). Data are shown as the means with S.E. The difference between control and N*Cmah*Tg mice was statistically significant when analyzed by two-tailed paired *t* test ($p < 0.001$). *G,* hot plate test. Latency to nociception response on a hot plate was recorded. $n = 6$ (control, N*Cmah*Tg). Data are shown as the means with S.E. *H,* MAG expression in the brain. Expression level of MAG and MBP, another myelin-resident protein, in 1-year-old *Cre*-positive control and N*Cmah*Tg mouse brains was examined by Western blotting. Data are representative of several independent experiments that yielded similar results. *Control*, wild-type or *Cre*-positive (no *Cmah* transgene); *Tg*, N*Cmah*Tg.

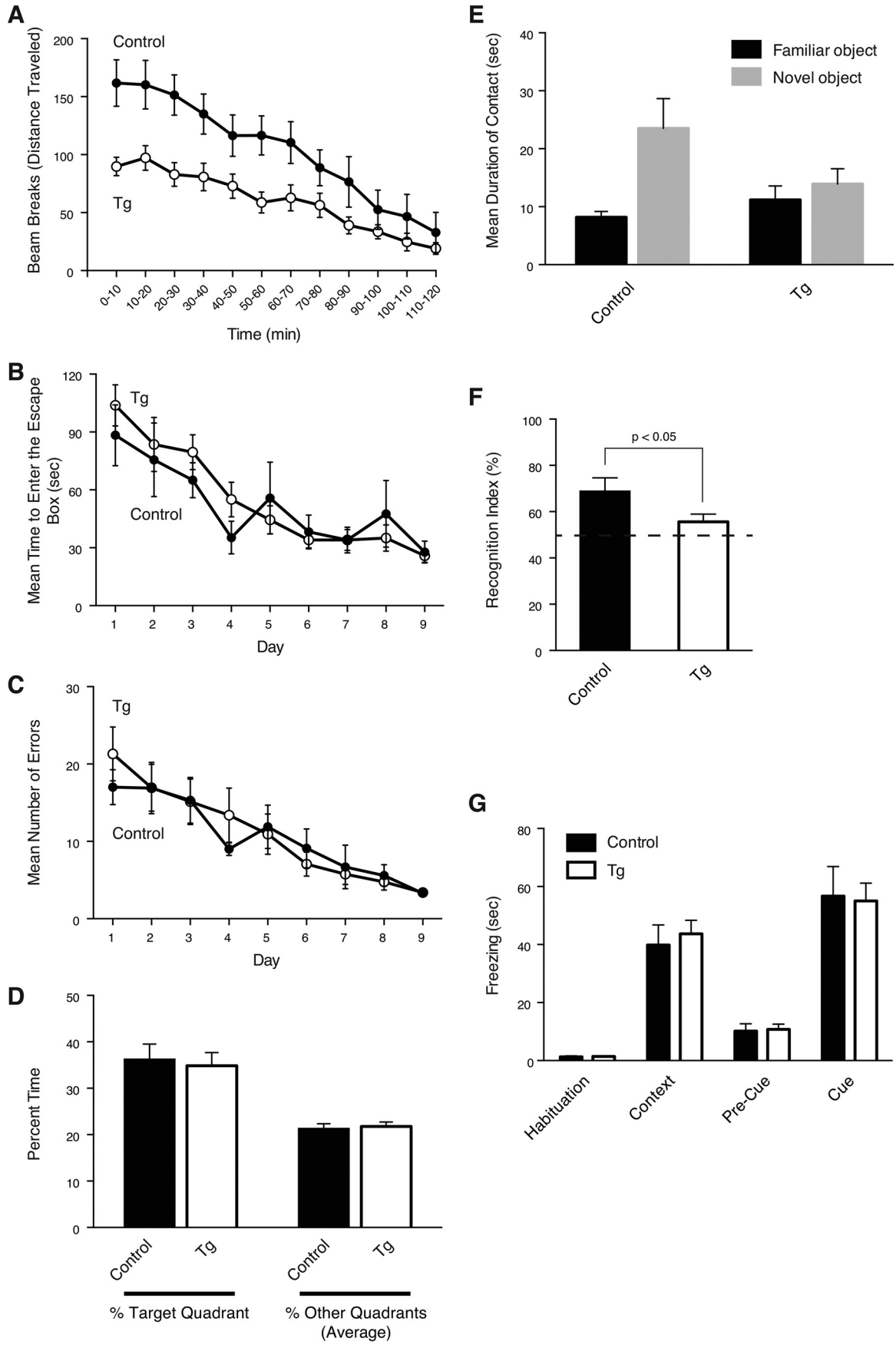
A
Beam Breaks (Distance Traveled)
Control
Tg
Time (min)
0-10
10-20
20-30
30-40
40-50
50-60
60-70
70-80
80-90
90-100
100-110
110-120
B
Mean Time to Enter the Escape Box (sec)
Tg
Control
Day
C
Mean Number of Errors
Tg
Control
Day
D
Percent Time
Control
Tg
Control
Tg
% Target Quadrant
% Other Quadrants (Average)
E
Mean Duration of Contact (sec)
Familiar object
Novel object
Control
Tg
F
Recognition Index (%)
p < 0.05
Control
Tg
G
Freezing (sec)
Control
Tg
Habituation
Context
Pre-Cue
Cue

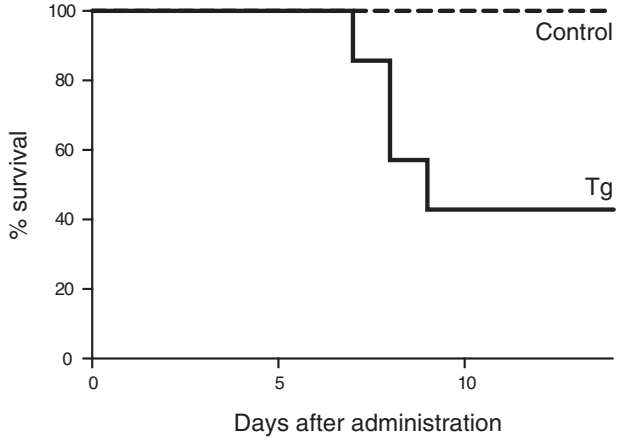

FIGURE 10. **Effect of brain expression of transgenic *Cmah* on sensitivity to a Neu5Gc-binding toxin.** SubAB toxin (2 μg/mouse) was intranasally administered to 5–7-month-old female mice. The survival rate was plotted. *Dashed line,* control (wild-type or *Cmah* transgene-positive (no *Cre*)); *solid line*, NC*mah*Tg mice. $n = 8$ (control) or 7 (NC*mah*Tg) in two independent experiments.

(sequentially stained), the brain sections after blocking were first incubated with anti-Neu5Gc antibody (1:2000 in 0.5% fish gelatin-containing PBS-T) for 2 h. Then antibody binding was visualized with biotinylated donkey anti-chicken IgY (1:500, Jackson ImmunoResearch), alkaline phosphatase-conjugated streptavidin (1:100, Jackson ImmunoResearch), and the VECTOR blue alkaline phosphatase substrate kit (Vector Laboratories). The antibody and probe were diluted in 0.5% fish gelatin-containing Tris-buffered saline with 0.1% Tween 20 (TBS-T), and incubation was done for 30–60 min at room temperature. After blocking with avidin-biotin blocking kit (Vector Laboratories) and 0.5% fish gelatin-containing PBS-T, the sections were stained with anti-CD31 (1:50, BD Biosciences) for 90 min, then with biotinylated goat anti-rat Ig (1:100, BD Biosciences) for 30 min, and horseradish peroxidase-conjugated streptavidin (1:500, Jackson ImmunoResearch) for 30 min. The antibodies and probe were diluted in 0.5% fish gelatin-containing PBS-T, and all incubation was done at room temperature. The antibody binding was visualized using AEC peroxidase substrate kit (Vector Laboratories).

For MAG-hFc staining, the brain sections were rehydrated in Tris-buffered saline (TBS), and nonspecific binding was blocked with 1% BSA in TBS. After fixation with 10% neutral buffered formalin for 30 min at room temperature, the sections were stained with MAG-Fc precomplexed with alkaline phosphatase-conjugated anti-human IgG (Jackson ImmunoResearch) (incubated in 1% BSA-containing TBS for 3 h at 4 °C) for more than 2 h at room temperature. MAG-Fc was prepared from culture supernatant of Lec2 stable cell line using protein A column. MAG-Fc binding was visualized using blue alkaline phosphatase substrate kit (Vector Laboratories) and cellular nuclei were counter stained with nuclear fast red.

High Performance Liquid Chromatography (HPLC)—Brain homogenate was subjected to acid hydrolysis with 2 M acetic acid for 3 h at 80 °C to release sialic acids from cellular glycoconjugates. After filtration using 10K Amicon Ultra (Millipore), the samples were mixed with equal amount of 2× DMB solution (7 mM 1,2-diamino-4,5-methylenedioxybenzene (DMB), 18 mM sodium hydrosulfite, 0.75 M 2-mercaptoethanol, 1.4 M acetic acid) and incubated for 2.5 h at 50 °C. The derivatized samples were analyzed on a reverse phase C18 column (Phenomenex) with an isocratic solvent composition of 7% methanol, 8% acetonitrile, 85% water using ELITE LaChrom system (Hitachi).

To analyze Neu5Gc incorporation into polySia, brains from postnatal day 2–3 mice were snap-frozen using liquid nitrogen and stored at −80 °C until use. The brains were homogenized in 10 mM Tris-HCl (pH 8.0) and subjected to delipidation (10 mM Tris-HCl (pH 8.0)/methanol/chloroform = 3:8:4 twice, ethanol, and then 70% ethanol). The delipidated samples were resuspended in 50 mM Tris-HCl (pH 8.0) and treated with EndoNF (kind gift from Dr. Rita Gerardy-Schahn, Hannover Medical School) for 1 h on ice. The released oligoSia fragments were collected as pass-through fraction of 3K Amicon Ultra (Millipore), hydrolyzed in 2 M acetic acid for 3 h at 80 °C, and derivatized with DMB as described above.

Western Blotting—Mouse brain was homogenized using Polytron in tissue lysis buffer (2% Triton X-100, 20 mM Tris-HCl (pH 8.0), 150 mM NaCl, 5 mM EDTA, and protease inhibitor cocktail (Calbiochem)) or TL lysis buffer (1% Triton X-100, 50 mM Tris-HCl (pH 7.6), 150 mM NaCl, 1 mM EDTA, and protease inhibitor cocktail (Calbiochem); for MAG and MBP detection) and incubated for 1 h on ice. Clear supernatant after centrifugation was collected as brain lysate. The obtained lysate was denatured in SDS-PAGE sample buffer (62.5 mM Tris-HCl (pH 6.8), 2% SDS, 10% glycerol, 5% β-mercaptoethanol, 0.005% bromphenol blue) for 5 min at 98 °C and then subjected to Western blotting. Protein bands were visualized using Odyssey infrared imager (LI-COR).

For analysis of NCAM polysialylation, the brain lysate samples were denatured in SDS-PAGE sample buffer for 10 min at 60 °C. EndoNF treatment was done for 1 h on ice before the denaturation. Samples for PNGase F treatment were first dena-

FIGURE 9. **Impaired locomotor activity and recognition memory in NC*mah*Tg mice (5–6 months old).** *A,* open field test. Locomotor activity for 2 h was plotted as beam breaks (traveled distance) per 10 min. *Open circles*, NC*mah*Tg mice; *filled circles*, control (*Cre*-positive (no *Cmah* transgene)) mice. Data are shown as the means with S.E. The difference between control and NC*mah*Tg mice was statistically significant when analyzed by two-tailed paired *t* test ($p < 0.001$). *B–D,* Barnes Maze test. Mean time to enter the escape box (*B*) and mean number of errors (*C*) were shown for 9 days of trials. On day 10, the escape box was removed, and time spent in each quadrant (target quadrant where the escape box was originally located and other three quadrants) was measured (*D*). Data are shown as the means with S.E. *Open circles*, NC*mah*Tg mice; *filled circles*, control (*Cre*-positive (no *Cmah* transgene)) mice. *E* and *F,* novel object recognition test. During two trials, two identical objects were placed in the testing chamber. Fifteen min later, one of the familiar objects was replaced with a novel object, and the duration of contact was measured. The result was shown as mean duration of contact (*E*) and recognition index (*F*) with S.E. Recognition index was calculated using the following formula: recognition index = (time exploring novel object/time exploring all objects) × 100. The difference in recognition index between control and NC*mah*Tg mice was statistically significant when analyzed by two-tailed unpaired *t* test. *G,* fear-conditioning test. Freezing behavior in each session was measured. Sessions: *Habituation*, conditioning chamber before conditioning; *Context,* trained chamber without the cue (light and tone); *Pre-Cue*, trained chamber with an altered context without the cue (light and tone); *Cue*, trained chamber with an altered context and cue (light and tone). Data are shown as the means with S.E. *Control, Cre*-positive (no *Cmah* transgene); *Tg*, NC*mah*Tg. $n = 10$ (control) or 16 (NC*mah*Tg).

tured for 10 min at 99 °C, incubated with PNGase F at 37 °C overnight, and then incubated in SDS-PAGE sample buffer for 5 min at 98 °C.

Antibodies used were as follows: anti-Cmah rabbit N8 antiserum (1:2500, kind gift from Dr. Yasunori Kozutsumi, Kyoto University); anti-actin (1:500) from Sigma; anti-Neu5Gc chicken IgY (1:3300) from BioLegend; anti-NCAM (H28-123, 1:200) and anti-MBP (1:100) from Santa Cruz Biotechnology; anti-poly Neu5Ac (12E3, 1 μg/ml, kind gift from Dr. Chihiro Sato, Nagoya University); anti-actin (1:1000) and anti-MAG (1:1000) from Cell Signaling; IRDye 800CW goat anti-rabbit IgG (1:15,000), IRDye 800CW goat anti-mouse IgG (1:15,000), IRDye 800CW donkey anti-chicken IgG (1:20,000), and IRDye 680RD goat anti-rat IgG (1:15,000) from LI-COR; and IRDye 800CW goat anti-mouse IgM (1:15,000) from Rockland.

Mass Spectrometry—Gangliosides were extracted from wild-type and N*Cmah*Tg mouse brains as described previously (58) and analyzed by MALDI-TOF/TOF instrument.

Imaging of Axon Myelination in Corpus Callosum and Sciatic Nerve—Mice were transcardially perfused with PBS and then 4% paraformaldehyde, 0.1% glutaraldehyde in PBS. Brains and sciatic nerves were removed and post-fixed in EM fixative (4% paraformaldehyde, 2% glutaraldehyde, 2.5% sucrose, 3 mM $CaCl_2$ in cacodylate-based buffer) on ice. Additional fixation was done with 2% osmium tetroxide. The tissue was stained en bloc with 2% uranyl acetate in distilled water for 30 min, dehydrated in graded ethanol, and embedded using Embed 812 (Electron Microscopy Sciences). For light microscopy, 1-μm sections were cut, captured on microscope slides, and stained with 1% toluidine blue. For electron microscopy, 70-nm-thin sections were cut using a Reichert Jung Ultracut E microtome and placed on Formvar-coated 100 mesh copper grids. The grids were stained with uranyl acetate followed by lead citrate. Imaging was performed on a Zeiss Libra 120 using an Olympus Veleta camera.

Hindlimb Reflex Extension—Each mouse was suspended by the tail for 30 s, and the reflex/position of the hindlimbs was scored double-blinded as follows (59): 0, one or both hindlimbs paralyzed; 1, loss of reflex and hindlimbs and paws held close to the body with clasping toes; 2, loss of reflex with flexion of hindlimbs; 3, hindlimbs extended to form $<$90 °C angle; 4, hindlimbs extended to form $>$90 °C angle. To assess severity, two more parameters were added to this hindlimb extension score as follows: whether they pulled legs close to the body and whether they could easily find stable position of hindlimbs during test time.

Gait Analysis—Gait measures were collected using an automated gait analysis system (CatWalk, Noldus Instruments). Mice were placed at the start of the runway and allowed to move to the end of the runway, where they can enter a dark enclosure. The test was performed once a day for 5 days. Measurements included stride length and stride width (front and hind).

Rotarod Test—A Roto-Rod Series 8 apparatus (Ugo Basile) was used. The rod was a knurled plastic dowel (6.0 cm diameter) set at a height of 30 cm, and the latencies to fall were automatically recorded by a computer. During training, the mice were placed on the stationary rotarod for 30 s before the trial was initiated. Then, each mouse was given three trials per day, with a 60-s intertrial interval on the accelerating rotarod (3–30 rpm over 5 min) for 3 consecutive days. The latency to fall was recorded for each trial.

Locomotor Activity—Locomotor activity was measured using an automated monitoring system (Kinder Associates). Polycarbonate cage (42 × 22 × 20 cm) containing a thin layer of bedding material was placed into frames (25.5 × 47 cm) mounted with photocell beams. Each mouse was tested for 1 or 2 h as indicated.

Hot Plate Test—Supraspinal antinociception was assessed by the hot plate method. Mice were placed on a hot plate (Thermostat Apparatus) maintained at 55 °C. Reaction time latency (jumping or paw licking) was recorded. A maximum latency of 40 s was imposed.

Barnes Maze Test—The Barnes maze used was an opaque Plexiglas® disc 75 cm in diameter elevated 58 cm above the floor by a tripod. Twenty holes, 5 cm in diameter, were located 5 cm from the perimeter, and a black Plexiglas® escape box (19 × 8 × 7 cm) was placed under one of the holes. Distinct spatial cues were located all around the maze and were kept constant throughout the study. On the 1st day of testing, a training session was performed, which consisted of placing the mouse in the escape box and leaving it there for 5 min. One min later, the first session was started. At the beginning of each session, the mouse was placed in the middle of the platform in a 10-cm high cylindrical black start chamber. After 10 s, the start chamber was removed, a light (400 lux) was turned on, and the mouse was allowed to freely explore the maze. The session ended when the mouse entered the escape box or after 3 min elapsed. When the mouse entered the escape box, the light was turned off and the mouse remained in the dark for 1 min. When the mouse did not enter the box by itself, it was gently put in the escape box for 1 min. The box was always located below the same hole (stable within the spatial environment), which is randomly determined for each mouse. Mice were tested once a day for 9 days. For the 10th test (probe test), the escape box was removed, and the mouse was allowed to freely explore the maze for 3 min. The time spent in each quadrant was determined, and the percent time spent in the target quadrant (the one originally containing the escape box) was compared with the average percent time in the other three quadrants.

Novel Object Exploration Test—All observations were conducted in a circular open field (80 cm in diameter) with walls (40 cm in height). The objects were a blue smooth metal rectangular can (7.5 × 4 × 13 cm) and a pink plastic cup (16 × 6.5 cm; tapered top). These objects could not be climbed and were of sufficient weight such that the mice could not move them. Testing consisted of three 6-min trials. During trials 1 and 2, two identical objects were placed in the field. Fifteen min after the second trial, the test session was performed. On the test, one of the familiar objects was replaced with a novel object to evaluate recognition memory. The number and the time spent in direct contact with the objects were recorded for 6 min.

Conditioned Fear Test—In this procedure, mice learn to associate a novel environment (context) and a previously neutral stimulus (conditioned stimulus, light, and tone) with an aversive foot shock stimulus. Testing occurred in the absence of the aversive stimulus. Once conditioned, animals will exhibit freez-

ing behavior when exposed to either the context in which the shock was received or to the conditioned stimulus. Conditioning was conducted using Freeze Monitor chambers (Med Associates) housed in soundproof boxes. On day 1, mice were placed in the conditioning chamber for 5 min to habituate them to the apparatus. On day 2, the mice were exposed to the context and conditioned stimulus (light and 30 s tone) in association with foot shock (0.70 mA, 2 s). On day 3, contextual conditioning (as determined by freezing behavior) was measured in a 5-min test in the chamber where the mice were trained (context test), and 4 h later the mice were tested for cued conditioning (conditioned stimulus + test). Freezing behavior in the context and cued tests (relative to the same context prior to shock and an altered context prior to tone, respectively) is indicative of the formation of an association between the particular stimulus (either the environment or the tone) and the shock, *i.e.* that learning has occurred.

Subtilase Cytotoxin (SubAB Toxin) Treatment—SubAB holotoxin, comprising the catalytic A subunit (a highly specific serine protease that cleaves the endoplasmic reticulum chaperone BiP/GRP78 (60)) and a pentameric B subunit specific for Neu5Gc with His_6 tags fused to the C termini, was purified from recombinant *Escherichia coli* using nickel-nitrilotriacetic acid chromatography, as described previously (61). The purified SubAB toxin stored in PBS, 50% glycerol was diluted in PBS, and 2 μg of SubAB toxin (5 μl by volume) was intranasally administered to 23–27-week-old female mice. The health condition/behavior was observed every day for more than 2 weeks.

Statistics—The statistical significance of the observed differences was evaluated using a paired or unpaired *t* test depending on the case unless otherwise specified. The numbers of mice used were more than the minimum required to detect statistical significance. Prism 6 Program (GraphPad) was used for the statistical analyses.

Author Contributions—Y. N.-M., L. R. L. D., H. T., A. F. C., C. J. H., and A. Varki designed the research. Y. N.-M., L. R. L. D., H. T., C. J. H., S.-W. Y., B. C., and R. L. S. performed the experiments. H.-H. C. and P. T. contributed to establish the transgenic mice. A. F. C. and A. Verhagen made plasmid constructs for the transgenic mice. N. M. V. supervised and interpreted the immunohistochemistry. J. C. P. and A. W. P. characterized and provided the functional SubAB toxin. Y. N.-M. and A. Varki wrote the manuscript. H. T., C. J. H., J. C. P., and R. L. S. reviewed the manuscript in detail.

Acknowledgments—We thank Dr. Akemi Suzuki (Tokai University) for ganglioside analysis, Dr. Shuichi Yamada (Kyoto University) for transgene injection to observe mouse embryos, Taishi Yuasa (Kyoto University) for preparation of MAG-Fc probe, and Sandra L. Diaz (University of California, San Diego) for helping to score hindlimb reflex.

References

1. Bernimoulin, M. P., Zeng, X. L., Abbal, C., Giraud, S., Martinez, M., Michielin, O., Schapira, M., and Spertini, O. (2003) Molecular basis of leukocyte rolling on PSGL-1. Predominant role of core-2 *O*-glycans and of tyrosine sulfate residue 51. *J. Biol. Chem.* **278,** 37–47
2. Poe, J. C., Fujimoto, Y., Hasegawa, M., Haas, K. M., Miller, A. S., Sanford, I. G., Bock, C. B., Fujimoto, M., and Tedder, T. F. (2004) CD22 regulates B lymphocyte function *in vivo* through both ligand-dependent and ligand-independent mechanisms. *Nat. Immunol.* **5,** 1078–1087
3. Varki, A. (2007) Glycan-based interactions involving vertebrate sialic acid-recognizing proteins. *Nature* **446,** 1023–1029
4. Freeze, H. H. (2013) Understanding human glycosylation disorders: biochemistry leads the charge. *J. Biol. Chem.* **288,** 6936–6945
5. Willems, A. P., van Engelen, B. G., and Lefeber, D. J. (2016) Genetic defects in the hexosamine and sialic acid biosynthesis pathway. *Biochim. Biophys. Acta* **1860,** 1640–1654
6. Schwarzkopf, M., Knobeloch, K. P., Rohde, E., Hinderlich, S., Wiechens, N., Lucka, L., Horak, I., Reutter, W., and Horstkorte, R. (2002) Sialylation is essential for early development in mice. *Proc. Natl. Acad. Sci. U.S.A.* **99,** 5267–5270
7. Varki, A., and Angata, T. (2006) Siglecs–the major subfamily of I-type lectins. *Glycobiology* **16,** 1R-27R
8. Crocker, P. R., Paulson, J. C., and Varki, A. (2007) Siglecs and their roles in the immune system. *Nat. Rev. Immunol.* **7,** 255–266
9. Kannagi, R. (2002) Regulatory roles of carbohydrate ligands for selectins in the homing of lymphocytes. *Curr. Opin. Struct. Biol.* **12,** 599–608
10. Byres, E., Paton, A. W., Paton, J. C., Löfling, J. C., Smith, D. F., Wilce, M. C., Talbot, U. M., Chong, D. C., Yu, H., Huang, S., Chen, X., Varki, N. M., Varki, A., Rossjohn, J., and Beddoe, T. (2008) Incorporation of a non-human glycan mediates human susceptibility to a bacterial toxin. *Nature* **456,** 648–652
11. Song, J., Gao, X., and Galán, J. E. (2013) Structure and function of the *Salmonella typhi* chimaeric A(2)B(5) typhoid toxin. *Nature* **499,** 350–354
12. Stencel-Baerenwald, J. E., Reiss, K., Reiter, D. M., Stehle, T., and Dermody, T. S. (2014) The sweet spot: defining virus-sialic acid interactions. *Nat. Rev. Microbiol.* **12,** 739–749
13. Schnaar, R. L., Gerardy-Schahn, R., and Hildebrandt, H. (2014) Sialic acids in the brain: gangliosides and polysialic acid in nervous system development, stability, disease, and regeneration. *Physiol. Rev.* **94,** 461–518
14. Inoue, S., and Inoue, Y. (2001) Developmental profile of neural cell adhesion molecule glycoforms with a varying degree of polymerization of polysialic acid chains. *J. Biol. Chem.* **276,** 31863–31870
15. Hildebrandt, H., Muhlenhoff, M., Weinhold, B., and Gerardy-Schahn, R. (2007) Dissecting polysialic acid and NCAM functions in brain development. *J. Neurochem.* **103,** Suppl. 1, 56–64
16. Rutishauser, U. (2008) Polysialic acid in the plasticity of the developing and adult vertebrate nervous system. *Nat. Rev. Neurosci.* **9,** 26–35
17. Franz, C. K., Rutishauser, U., and Rafuse, V. F. (2005) Polysialylated neural cell adhesion molecule is necessary for selective targeting of regenerating motor neurons. *J. Neurosci.* **25,** 2081–2091
18. Sato, C., and Kitajima, K. (2013) Disialic, oligosialic and polysialic acids: distribution, functions and related disease. *J. Biochem.* **154,** 115–136
19. Sumida, M., Hane, M., Yabe, U., Shimoda, Y., Pearce, O. M., Kiso, M., Miyagi, T., Sawada, M., Varki, A., Kitajima, K., and Sato, C. (2015) Rapid trimming of cell surface polysialic acid (polySia) by exovesicular sialidase triggers release of preexisting surface neurotrophin. *J. Biol. Chem.* **290,** 13202–13214
20. Isomura, R., Kitajima, K., and Sato, C. (2011) Structural and functional impairments of polysialic acid by a mutated polysialyltransferase found in schizophrenia. *J. Biol. Chem.* **286,** 21535–21545
21. Sato, C., and Kitajima, K. (2013) Impact of structural aberrancy of polysialic acid and its synthetic enzyme ST8SIA2 in schizophrenia. *Front. Cell Neurosci.* **7,** 61
22. Kamien, B., Harraway, J., Lundie, B., Smallhorne, L., Gibbs, V., Heath, A., and Fullerton, J. M. (2014) Characterization of a 520 kb deletion on chromosome 15q26.1 including ST8SIA2 in a patient with behavioral disturbance, autism spectrum disorder, and epilepsy. *Am. J. Med. Genet. A* **164A,** 782–788
23. Shaw, A. D., Tiwari, Y., Kaplan, W., Heath, A., Mitchell, P. B., Schofield, P. R., and Fullerton, J. M. (2014) Characterisation of genetic variation in ST8SIA2 and its interaction region in NCAM1 in patients with bipolar disorder. *PLoS ONE* **9,** e92556
24. Varki, A. (1992) Diversity in the sialic acids. *Glycobiology* **2,** 25–40

25. Shaw, L., and Schauer, R. (1988) The biosynthesis of *N*-glycoloylneuraminic acid occurs by hydroxylation of the CMP-glycoside of *N*-acetylneuraminic acid. *Biol. Chem. Hoppe Seyler* **369,** 477–486
26. Kawano, T., Koyama, S., Takematsu, H., Kozutsumi, Y., Kawasaki, H., Kawashima, S., Kawasaki, T., and Suzuki, A. (1995) Molecular cloning of cytidine monophospho-*N*-acetylneuraminic acid hydroxylase. Regulation of species- and tissue-specific expression of *N*-glycolylneuraminic acid. *J. Biol. Chem.* **270,** 16458–16463
27. Higa, H. H., and Paulson, J. C. (1985) Sialylation of glycoprotein oligosaccharides with *N*-acetyl-, *N*-glycolyl-, and *N*-*O*-diacetylneuraminic acids. *J. Biol. Chem.* **260,** 8838–8849
28. Lepers, A., Shaw, L., Schneckenburger, P., Cacan, R., Verbert, A., and Schauer, R. (1990) A study on the regulation of *N*-glycoloylneuraminic acid biosynthesis and utilization in rat and mouse liver. *Eur. J. Biochem.* **193,** 715–723
29. Tsuji, S. (1996) Molecular cloning and functional analysis of sialyltransferases. *J. Biochem.* **120,** 1–13
30. Davies, L. R., Pearce, O. M., Tessier, M. B., Assar, S., Smutova, V., Pajunen, M., Sumida, M., Sato, C., Kitajima, K., Finne, J., Gagneux, P., Pshezhetsky, A., Woods, R., and Varki, A. (2012) Metabolism of vertebrate amino sugars with *N*-glycolyl groups: resistance of α2–8-linked *N*-glycolylneuraminic acid to enzymatic cleavage. *J. Biol. Chem.* **287,** 28917–28931
31. Davies, L. R., and Varki, A. (2015) Why is *N*-glycolylneuraminic acid rare in the vertebrate brain. *Top. Curr. Chem.* **366,** 31–54
32. Diaz, S. L., Padler-Karavani, V., Ghaderi, D., Hurtado-Ziola, N., Yu, H., Chen, X., Brinkman-Van der Linden, E. C., Varki, A., and Varki, N. M. (2009) Sensitive and specific detection of the non-human sialic acid *N*-glycolylneuraminic acid in human tissues and biotherapeutic products. *PLoS ONE* **4,** e4241
33. Forss-Petter, S., Danielson, P. E., Catsicas, S., Battenberg, E., Price, J., Nerenberg, M., and Sutcliffe, J. G. (1990) Transgenic mice expressing beta-galactosidase in mature neurons under neuron-specific enolase promoter control. *Neuron* **5,** 187–197
34. Hoesche, C., Sauerwald, A., Veh, R. W., Krippl, B., and Kilimann, M. W. (1993) The 5′-flanking region of the rat synapsin I gene directs neuron-specific and developmentally regulated reporter gene expression in transgenic mice. *J. Biol. Chem.* **268,** 26494–26502
35. Zhu, Y., Romero, M. I., Ghosh, P., Ye, Z., Charnay, P., Rushing, E. J., Marth, J. D., and Parada, L. F. (2001) Ablation of NF1 function in neurons induces abnormal development of cerebral cortex and reactive gliosis in the brain. *Genes Dev.* **15,** 859–876
36. Tronche, F., Kellendonk, C., Kretz, O., Gass, P., Anlag, K., Orban, P. C., Bock, R., Klein, R., and Schütz, G. (1999) Disruption of the glucocorticoid receptor gene in the nervous system results in reduced anxiety. *Nat. Genet.* **23,** 99–103
37. Lakso, M., Pichel, J. G., Gorman, J. R., Sauer, B., Okamoto, Y., Lee, E., Alt, F. W., and Westphal, H. (1996) Efficient *in vivo* manipulation of mouse genomic sequences at the zygote stage. *Proc. Natl. Acad. Sci. U.S.A.* **93,** 5860–5865
38. Brinster, R. L., Chen, H. Y., Warren, R., Sarthy, A., and Palmiter, R. D. (1982) Regulation of metallothionein-thymidine kinase fusion plasmids injected into mouse eggs. *Nature* **296,** 39–42
39. Takematsu, H., Kawano, T., Koyama, S., Kozutsumi, Y., Suzuki, A., and Kawasaki, T. (1994) Reaction mechanism underlying CMP-N-acetylneuraminic acid hydroxylation in mouse liver: formation of a ternary complex of cytochrome b5, CMP-*N*-acetylneuraminic acid, and a hydroxylation enzyme. *J. Biochem. (Tokyo)* **115,** 381–386
40. Finne, J., Finne, U., Deagostini-Bazin, H., and Goridis, C. (1983) Occurrence of α2–8 linked polysialosyl units in a neural cell adhesion molecule. *Biochem. Biophys. Res. Commun.* **112,** 482–487
41. Galuska, S. P., Rollenhagen, M., Kaup, M., Eggers, K., Oltmann-Norden, I., Schiff, M., Hartmann, M., Weinhold, B., Hildebrandt, H., Geyer, R., Mühlenhoff, M., and Geyer, H. (2010) Synaptic cell adhesion molecule SynCAM 1 is a target for polysialylation in postnatal mouse brain. *Proc. Natl. Acad. Sci. U.S.A.* **107,** 10250–10255
42. Schnaar, R. L., and Lopez, P. H. (2009) Myelin-associated glycoprotein and its axonal receptors. *J. Neurosci. Res.* **87,** 3267–3276
43. Collins, B. E., Fralich, T. J., Itonori, S., Ichikawa, Y., and Schnaar, R. L. (2000) Conversion of cellular sialic acid expression from *N*-acetyl- to *N*-glycolylneuraminic acid using a synthetic precursor, *N*-glycolylmannosamine pentaacetate: inhibition of myelin-associated glycoprotein binding to neural cells. *Glycobiology* **10,** 11–20
44. Blixt, O., Collins, B. E., van den Nieuwenhof, I. M., Crocker, P. R., and Paulson, J. C. (2003) Sialoside specificity of the Siglec family assessed using novel multivalent probes: identification of potent inhibitors of myelin associated glycoproteins. *J. Biol. Chem.* **278,** 31007–31019
45. Stiles, T. L., Dickendesher, T. L., Gaultier, A., Fernandez-Castaneda, A., Mantuano, E., Giger, R. J., and Gonias, S. L. (2013) LDL receptor-related protein-1 is a sialic-acid-independent receptor for myelin-associated glycoprotein that functions in neurite outgrowth inhibition by MAG and CNS myelin. *J. Cell Sci.* **126,** 209–220
46. Li, C., Tropak, M. B., Gerlai, R., Clapoff, S., Abramow-Newerly, W., Trapp, B., Peterson, A., and Roder, J. (1994) Myelination in the absence of myelin-associated glycoprotein. *Nature* **369,** 747–750
47. Yin, X., Crawford, T. O., Griffin, J. W., Tu, Ph, Lee, V. M., Li, C., Roder, J., and Trapp, B. D. (1998) Myelin-associated glycoprotein is a myelin signal that modulates the caliber of myelinated axons. *J. Neurosci.* **18,** 1953–1962
48. Sheikh, K. A., Sun, J., Liu, Y., Kawai, H., Crawford, T. O., Proia, R. L., Griffin, J. W., and Schnaar, R. L. (1999) Mice lacking complex gangliosides develop Wallerian degeneration and myelination defects. *Proc. Natl. Acad. Sci. U.S.A.* **96,** 7532–7537
49. Pan, B., Fromholt, S. E., Hess, E. J., Crawford, T. O., Griffin, J. W., Sheikh, K. A., and Schnaar, R. L. (2005) Myelin-associated glycoprotein and complementary axonal ligands, gangliosides, mediate axon stability in the CNS and PNS: Neuropathology and behavioral deficits in single- and double-null mice. *Exp. Neurol.* **195,** 208–217
50. Takamiya, K., Yamamoto, A., Furukawa, K., Yamashiro, S., Shin, M., Okada, M., Fukumoto, S., Haraguchi, M., Takeda, N., Fujimura, K., Sakae, M., Kishikawa, M., Shiku, H., Furukawa, K., and Aizawa, S. (1996) Mice with disrupted GM2/GD2 synthase gene lack complex gangliosides but exhibit only subtle defects in their nervous system. *Proc. Natl. Acad. Sci. U.S.A.* **93,** 10662–10667
51. Sun, J., Shaper, N. L., Itonori, S., Heffer-Lauc, M., Sheikh, K. A., and Schnaar, R. L. (2004) Myelin-associated glycoprotein (Siglec-4) expression is progressively and selectively decreased in the brains of mice lacking complex gangliosides. *Glycobiology* **14,** 851–857
52. Wan, H., Aggleton, J. P., and Brown, M. W. (1999) Different contributions of the hippocampus and perirhinal cortex to recognition memory. *J. Neurosci.* **19,** 1142–1148
53. Brown, M. W., and Aggleton, J. P. (2001) Recognition memory: what are the roles of the perirhinal cortex and hippocampus. *Nat. Rev. Neurosci.* **2,** 51–61
54. Xiao, C., Davis, F. J., Chauhan, B. C., Viola, K. L., Lacor, P. N., Velasco, P. T., Klein, W. L., and Chauhan, N. B. (2013) Brain transit and ameliorative effects of intranasally delivered anti-amyloid-β oligomer antibody in 5XFAD mice. *J. Alzheimers Dis.* **35,** 777–788
55. Svennerholm, L. (1956) Composition of gangliosides from human brain. *Nature* **177,** 524–525
56. Tettamanti, G., Bertona, L., Berra, B., and Zambotti, V. (1965) Glycolylneuraminic acid in ox brain gangliosides. *Nature* **206,** 192–192
57. Muto, J., Morioka, Y., Yamasaki, K., Kim, M., Garcia, A., Carlin, A. F., Varki, A., and Gallo, R. L. (2014) Hyaluronan digestion controls DC migration from the skin. *J. Clin. Invest.* **124,** 1309–1319
58. Sturgill, E. R., Aoki, K., Lopez, P. H., Colacurcio, D., Vajn, K., Lorenzini, I., Majić, S., Yang, W. H., Heffer, M., Tiemeyer, M., Marth, J. D., and Schnaar, R. L. (2012) Biosynthesis of the major brain gangliosides GD1a and GT1b. *Glycobiology* **22,** 1289–1301
59. Chiavegatto, S., Sun, J., Nelson, R. J., and Schnaar, R. L. (2000) A functional role for complex gangliosides: Motor deficits in GM2/GD2 synthase knockout mice. *Exp. Neurol.* **166,** 227–234
60. Paton, A. W., Beddoe, T., Thorpe, C. M., Whisstock, J. C., Wilce, M. C., Rossjohn, J., Talbot, U. M., and Paton, J. C. (2006) AB5 subtilase cytotoxin inactivates the endoplasmic reticulum chaperone BiP. *Nature* **443,** 548–552
61. Paton, A. W., Srimanote, P., Talbot, U. M., Wang, H., and Paton, J. C. (2004) A new family of potent AB(5) cytotoxins produced by Shiga toxigenic *Escherichia coli*. *J. Exp. Med.* **200,** 35–46